BUTTERWORTH HEINEMANN

0016-2361(95)00170-0

Fuel Vol. 74 No. 12, pp. 1891–1902, 1995

0016-2361/95/$9.50 + 0.00

Easily computable good approximations for spectral radiative properties of particle–gas components and mixture in pulverized coal combustors

Changsik Kim and Noam Lior
Department of Mechanical Engineering and Applied Mechanics, University of Pennsylvania, Philadelphia, PA 19104-6315, USA
(Received 17 May 1994; revised 21 April 1995)

A rather large computational effort is required for calculating the exact values of the spectral radiative extinction, absorption and scattering coefficients in pulverized coal combustors, which contain a polydispersed solid–gas mixture of reactants and combustion products (coal, char, fly ash and soot particles and gaseous components). This computation becomes an especially significant problem in comprehensive modelling of coal combustors, where these properties vary in space and time and where the solution methods are iterative. A number of approximate expressions for calculating these coefficients for each of the particle types, requiring practically insignificant computational effort, are examined for a wide range of size parameters, by comparison with the results of the full Mie equations solved with Mathematica. A set of these approximations, which typically produce errors of <8.9% and <5.1% in the spectral extinction and scattering coefficients respectively, is recommended for use. The spectral absorption coefficient for the gas components is obtained by using the exponential wide-band model. A solution of a comprehensive model of a pulverized anthracite coal combustor shows that the combined error introduced by the recommended radiative property approximations generates an error of <1.45% in the combustor gas temperature and radiation intensity profile predictions.

(Keywords: pulverized coal combustion; spectral radiative properties; computation)

The medium in a pulverized coal combustor is inhomogeneous and participates significantly in the radiative heat transfer. It is a polydispersed mixture of reactant and combustion product gases and of solid particles consisting of coal, char, fly ash and soot, which emit, absorb and anisotropically scatter radiant energy. Owing to their different sizes and optical properties, each type of solid particle has different radiative properties. Furthermore, these properties vary for each particle as its temperature, size and shape change during its travel through the combustor.

The radiative properties of the particles in the particle–gas mixture can be obtained from electromagnetic theory. Although theoretical solutions were derived long ago by Mie[1], reliable algorithms for computing them for arbitrary size parameters and refractive indices became available only relatively recently[2,3]. Despite the great advance in computation effectiveness, the formidable Mie equations still need significant computational effort, especially when used in models where the radiative properties vary in space and time. Since computational schemes for the solution of problems in which these properties are used are typically iterative, the effort is enormously compounded and therefore a simplified approximation is highly desirable.

Among authors concerned with the radiation by particulates in coal combustors, Tien *et al.*[4] derived a simple formula for the extinction coefficient of carbon smoke by using approximate expressions for the radiation efficiency factor. However, its utility is limited to particles for which the complex indices satisfy the condition $n - 1 \approx nk$. Buckius and Hwang[5] analysed the extinction and absorption coefficients for polydispersed absorbing particles. They used a downward recurrence relation to calculate the infinite series of Riccati–Bessel functions that was obtained from the Mie scattering theory. They also derived an empirical equation for spectral properties of coal that was based on the asymptotic behaviour at small and large size parameters, which makes its applicability limited. Viskanta *et al.*[6] calculated the spectral coefficients for pulverized coal and fly ash by the same method as Buckius and Hwang[5], computing the efficiency factors directly from the series expressions. Although the calculation procedure in these two studies is straightforward, the approach of direct calculation from the Mie equations is impractically time-consuming for inhomogeneous media in which the radiation properties vary in space and time. Wall *et al.*[7] used the mean absorption efficiency factor to calculate the absorption

coefficient. However, this factor had to be determined by using empirical absorption coefficients. Specifically for the conditions in the early pyrolysis zone in coal combustors, Grosshandler and Monteiro[8] obtained an empirical equation for the spectral absorptivity of coal and char particles of size 50–150 μm, with 5% accuracy in the 1.2–5.3 μm region. In the large size parameter limit, pertinent to these conditions, the absorption coefficient was then determined from the absorptivity. By applying the anomalous diffraction limit[9] (called the 'anomalous limit' here), Mengüç and Viskanta[10] obtained closed-form expressions for the spectral extinction and absorption coefficients of coal particles in a combustor. The validity of the approximation however is limited to the particle for which the refractive indices are near 1 and the absorptive indices near 0. Among the particulates found in a coal combustor, only ash particles have such small refractive indices.

This paper uses a simplified set of equations to describe the radiative properties of a particle–gas mixture typical of the medium in pulverized coal combustors, and determines the error in their use by comparison with results from the exact models. It thereby gives recommendations for specific simplified equations that can be used in the computation of the radiative properties of such media.

RADIATIVE PROPERTIES OF PARTICLE–GAS MIXTURES

Radiative properties of gas components

It is well established that of the several gas components in a pulverized coal combustor, water vapour and carbon dioxide are the major absorbers/emitters of radiant energy. Although other gases such as NO, SO_2, CO and hydrocarbons exist and may have some localized influence, their overall contribution to flame emission in a large combustor or boiler is relatively small (e.g. <0.2% for NO and 2–4% for SO_2; the CO absorption band is much weaker than those of CO_2 and H_2O, and its concentration is low, as it is converted to CO_2) and usually neglected[11].

Owing to the transition between discrete energy levels, absorption and emission by gas species are important only in certain wavelength regions. The primary infrared bands considered in this study are those at 1.38, 1.87, 2.7 and 6.3 μm, as well as the pure rotational band, for H_2O, and 2.7, 4.3 and 15 μm for CO_2[12,13].

Radiative properties of gases are best evaluated by considering their exact spectral description, or almost as well by the use of narrow-band models. However, such models require tedious and time-consuming calculation procedures. Wide-band models are much easier to apply and typically yield sufficiently accurate results in practical applications; Mengüç[14] for example has shown that the Planck mean absorption coefficients calculated by the exponential wide-band model are higher by only 3.64% and 6.67% at 1000 and 2000 K respectively (at $P = 1$ atm, $p_{CO2} = p_{H2O} = 0.1$ atm) than those calculated by the narrow-band model. Tiwari[15] applied wide-band models to realistic problems and justified their use for gases such as CO_2. Consequently, in this study, the wide-band model with an exponentially decaying band shape is used to calculate absorption coefficients of the gas components. Scattering by the gas molecules is neglected.

For just-overlapping lines, the spectral absorption coefficient for the gas component is expressed as[16–18]

$$\kappa = \rho \sum_{i=1}^{N} \frac{\alpha_i(T)}{\omega_i(T)} \exp\left[-t\frac{|\nu_i - \nu|}{\omega_i(T)}\right] \quad (1)$$

where N is the number of bands considered, $t = 1$ for bands which have head (i.e. asymmetric) bands and $t = 2$ for symmetric bands. In this expression, ρ is the mass density of gas components, α_i is the integrated intensity of the ith band, ω_i is the band wing decay width and ν_i is the band head for the asymmetric bands and the band centre for the symmetric ones. This expression gives accurate results if there is a considerable line overlap, i.e. in optically thick situations. The expressions for α_i and ω_i and the parameters needed can be found elsewhere[12,13,19] and are not repeated here.

Radiative properties of polydispersed particles

Mie scattering theory and radiative properties. Scattering depends on the optical properties of particles (i.e. the complex refractive index, $m = n - ik$) and the size parameter ($x = \pi d/\lambda$). Although the particles found in a coal combustor are of irregular shape, the effect of irregularity on the radiation characteristics is negligible if a proper size distribution model is used[9,20,21]. Such a model was indeed used here (see Particle size distribution, below) and it has consequently been assumed that all the particles are spherical.

Usually four different types of polydisperse particles exist in a coal combustor: pulverized coal, char, fly ash and soot. As devolatilization is completed, a char particle consisting of carbon and mineral matter is produced from a coal particle. This solid carbon is consumed by heterogeneous reaction with oxygen, leaving only mineral matter if combustion is complete. In fact, the char particle structure weakens during burnout and consequently fractures. If combustion is not complete, the resulting ash particles may be still bound with some unburnt carbon. However, it is not clear when the break-up occurs: Flagan[22] suggested that it occurs at 90% burnout, but here the assumption of Smoot and Pratt[23] is adopted, that fragmentation does not occur until carbon consumption is complete. As combustion proceeds, spherical ash droplets are formed from coalescing mineral matter. It is assumed here that upon completion of char combustion, the ash breaks into several pieces, depending on the chemical composition and combustion conditions, and contributes to radiation. Throughout the combustion process, hot particles of spherical or filamentous carbon (soot) are formed by incomplete combustion. Soot emits radiation over a continuous spectrum and is a very important radiating component, as is confirmed below.

By assuming single, independent scattering, the radiative properties of a medium containing polydispersed particles can be obtained from[24]

$$\eta(m, N, \lambda) = \int_0^\infty \pi r^2 Q_\eta(m, r, \lambda) n(r) \mathrm{d}r \quad (2)$$

where η denotes either the extinction (β), the scattering (σ) or the absorption (κ) coefficient. In this expression, Q_η is the corresponding radiation efficiency factor, m

is the complex refractive index of the particles, N is the particle number density, λ is the wavelength, r is the particle radius and $n(r)$ is the particle size distribution function.

The extinction and scattering efficiency factors, Q_β and Q_σ, derived from the Mie theory are an infinite series of a function of the Mie coefficients a_n and b_n[9]:

$$Q_\beta = \frac{2}{x^2}\sum_{n=1}^{\infty}(2n+1)\mathrm{Re}(a_n + b_n) \tag{3}$$

$$Q_\sigma = \frac{2}{x^2}\sum_{n=1}^{\infty}(2n+1)(|a_n|^2 + |b_n|^2) \tag{4}$$

where a_n and b_n are

$$a_n = \frac{\psi_n'(mx)\psi_n(x) - m\psi_n(mx)\psi_n'(x)}{\psi_n'(mx)\zeta_n(x) - m\psi_n(mx)\zeta_n'(x)} \tag{5}$$

$$b_n = \frac{m\psi_n'(mx)\psi_n(x) - \psi_n(mx)\psi_n'(x)}{m\psi_n'(mx)\zeta_n(x) - \psi_n(mx)\zeta_n'(x)} \tag{6}$$

where $\psi(x)$ and $\zeta(x)$ are the Riccati–Bessel functions, which are defined by the Bessel (J) and Hankel (H) functions as

$$\psi_n(z) = (\pi z/2)^{1/2}J_{n+1/2}(z) \tag{7}$$

$$\zeta_n(z) = (\pi z/2)^{1/2}H^{(2)}_{n+1/2}(z) \tag{8}$$

The radiative efficiency factor. As discussed above, the calculation of the efficiency factors has been quite complicated and time-consuming. Although the direct solution of the Mie equations became much easier and straightforward with the advance in computers and algorithms[2,3,25], the associated effort in iterative field modelling of combustors is still rather substantial, and simplified approximations are highly desirable. Such approximations have been derived for a number of limiting cases of the size parameter and the complex refractive index[9], and are examined here for suitability for the particles existing in a pulverized coal combustor, as follows.

(1) *Coal and char particles.* For pulverized coal, typically having an average diameter of the order of 100 μm, and for the char particles which retain the same order of diameter, and for the wavelengths of 1–10 μm which pertain to the conditions in typical coal combustors, the size parameter x is very large, of the order of 10π–100π. The complex refractive index of the coal and char particles is in the range ~1.6–3.6 at $\lambda = 2\,\mu$m. For such large values of $x(\gg 1)$ with $|m| > 2$, an asymptotic approximation to the efficiency factors, called the 'geometrical limit', was found quite suitable[9]. It is given by

$$Q_\beta(x,m) = 2 \tag{9}$$

$$Q_\kappa(x,m) = \tfrac{1}{2}(f_1 + f_2) \tag{10}$$

where

$$f_i = \frac{8}{q_i^2}[q_i - \ln(1 + q_i + \tfrac{1}{2}q_i^2)], \quad i = 1,2 \tag{11}$$

with

$$q_1 = (nk)^{-1/2} \quad \text{and} \quad q_2 = 2/q_1 \tag{12}$$

(2) *Fly ash particles.* As a result of char fragmentation, each char particle breaks up into typically three (from 75–90 μm lignite) to five (from 38–45 μm bituminous coal) ash particles 10–30 μm in diameter, and 200–500 fine ash particles 1–10 μm in diameter (10–20% of the total ash mass)[26,27]. When the oxygen concentration is <8%, the mass of the fly ash particles in the 1–5 μm size range is almost zero[28].

The typical size parameter of an ash particle at $\lambda = 2\,\mu$m is thus of the order of 10, i.e. $x \gg 1$. The refractive index for fly ash is near 1 (i.e. $|m-1| \ll 1$). A good approximation to the efficiency factors for these conditions has been shown[9] to be the 'anomalous limit',

$$\begin{aligned} Q_\beta(x,m) = 2 &- 4\mathrm{e}^{-\rho\tan\phi}\left(\frac{\cos\phi}{\rho}\right)\sin(\rho-\phi) \\ &- 4\mathrm{e}^{-\rho\tan\phi}\left(\frac{\cos\phi}{\rho}\right)^2\cos(\rho-2\phi) \\ &+ 4\left(\frac{\cos\phi}{\rho}\right)^2\cos 2\phi \end{aligned} \tag{13}$$

$$Q_\kappa(x,m) = 1 + \frac{\mathrm{e}^{-4xk}}{2xk} + \frac{(\mathrm{e}^{-4xk}-1)}{8x^2k^2} \tag{14}$$

where

$$\rho = 2x(n-1) \quad \text{and} \quad \phi = \tan^{-1}\left(\frac{k}{n-1}\right) \tag{15}$$

The expression for the extinction efficiency factor can be simplified further for non-absorbing spheres ($k = 0$, the 'dielectric limit') as

$$Q_\beta(x,m) = 2 - \frac{4\sin\rho}{\rho} + \frac{4(1-\cos\rho)}{\rho^2} \tag{16}$$

Since the imaginary part of the refractive index of fly ash is very small (of the order of 0.01)[29,30], either Equation (13) or Equation (16) can be used for calculating the extinction coefficient of fly ash.

(3) *Soot particles.* The typical size of soot particles in a coal combustor is in the range 0.02–0.06 μm, making their size parameter <0.2. For particles of such small size parameter, the general Mie solution can be expanded into a power series in terms of x. By expanding the leading Mie coefficients a_1, a_2, a_3, b_1 and b_2 in a series, Penndorf[31] approximated the efficiency factors as

$$Q_\beta(x,m) = c_1x + c_2x^2 + c_3x^4 \tag{17}$$

$$Q_\kappa(x,m) = c_1x + c_2x^3 + c_4x^4 + c_5x^6 + c_6x^7 \tag{18}$$

where the constants c_i are given by

$$c_1 = \left\{\frac{24kn}{4k^2n^2 + (2-k^2+n^2)^2}\right\} \tag{19}$$

$$\begin{aligned} c_2 = 4kn\Bigg\{&\frac{1}{15} + \frac{5}{3}\frac{1}{16k^2n^2 + [3+2(-k^2+n^2)]^2} \\ &+ \frac{6}{5}\frac{[7(k^2+n^2)^2 + 4(-5-k^2+n^2)]}{[4k^2n^2 + (2-k^2+n^2)^2]^2}\Bigg\} \end{aligned} \tag{20}$$

$$c_3 = \frac{8}{3}\left\{1 + \frac{(1+k^2+n^2)^2 - 4n^2}{4k^2n^2 + (2-k^2+n^2)^2} + \frac{[-2-k^2-n^2+(k^2+n^2)^2]^2 - 36k^2n^2}{[4k^2n^2 + (2-k^2+n^2)^2]^2}\right\} \quad (21)$$

$$c_4 = \frac{8}{3}\left\{1 - \frac{(1+k^2+n^2)^2 - 4n^2}{4k^2n^2 + (2-k^2+n^2)^2}\right\} \quad (22)$$

$$c_5 = -\frac{16}{5}\left\{\frac{[(k^2+n^2)^2 - 4][(1+k^2+n^2)^2 - 4n^2]}{[4k^2n^2 + (2-k^2+n^2)^2]^2}\right\} \quad (23)$$

$$c_6 = -\frac{32}{3}\left\{\frac{2kn[(1+k^2+n^2)^2 - 4n^2]}{[4k^2n^2 + (2-k^2+n^2)^2]^2}\right\} \quad (24)$$

The set of Equations (17)–(24) can be called the Penndorf approximation.

Particle size distribution. To integrate Equation (2), an expression for the particle size distribution is needed. Inclusion of a proper distribution function is also known to reduce the effect of irregular particle shape on the properties. The gamma distribution formula[32] is used in this study:

$$n(r) = ar^{\alpha}e^{-br} \quad (25)$$

By integrating the distribution function over all size ranges, the size-distribution coefficient a is obtained as

$$a = \frac{Nb^{\alpha+1}}{\Gamma(\alpha+1)} \quad (26)$$

The exponent b is found from the condition of extremum at the most probable (modal) particle size r_m,

$$b = \frac{\alpha}{r_m} \quad (27)$$

where α is determined from experimental data. This size distribution is used not only because of its popularity but also because it is directly integrable and thus amenable to this study's objective, the development of easily computable approximations of radiative properties. For example, the more appropriate distributions in the work of Dunn-Rankin and Kerstein[33] do not provide such an expression.

Simplified expressions for the radiative properties. Substituting the size distribution function, Equations (25)–(27), and the simplified expressions for the efficiency factors into Equation (2), the spectral extinction and absorption coefficients of the various solid particles can be found. The resulting extinction and absorption coefficients, non-dimensionalized with respect to the overall mean radius defined as

$$\bar{r} = \frac{\int_0^\infty n(r)r\,dr}{\int_0^\infty n(r)\,dr} = \frac{1}{N}\int_0^\infty n(r)r\,dr = \frac{\alpha+1}{b} = \frac{\alpha+1}{\alpha}r_m \quad (28)$$

are obtained for each of the particle types in a pulverized coal combustor as follows.

(1) *For coal and char particles.* Using the 'geometrical limit' approximation of the efficiency factors, Equations (9) and (10), the expressions for the dimensionless extinction and absorption coefficients for large coal and char particles are

$$\beta^*(m,\lambda) = \frac{\beta(m,\lambda)}{N\pi\bar{r}^2} = \frac{2a\Gamma(\alpha+3)}{N\bar{r}^2 b^{\alpha+3}} \quad (29)$$

$$\kappa^*(m,\lambda) = \frac{\kappa(m,\lambda)}{N\pi\bar{r}^2} = \frac{a(f_1+f_2)}{2N\bar{r}^2}\frac{\Gamma(\alpha+3)}{b^{\alpha+3}}. \quad (30)$$

(2) *For fly ash.* Application of the 'anomalous limit', Equations (13) and (14), to fly ash gives the dimensionless coefficients

$$\beta^*(m,\lambda) = \frac{a}{N\bar{r}^2}\left\{\frac{2\Gamma(\alpha+3)}{b^{\alpha+3}} - \frac{4\cos\phi\sin[(\alpha+2)\psi-\phi]\Gamma(\alpha+2)}{C_1^{\alpha+3}(C_2^2+1)^{(\alpha+2)/2}} - \frac{4\cos^2\phi\cos[(\alpha+1)\psi-\phi]\Gamma(\alpha+1)}{C_1^{\alpha+3}(C_2^2+1)^{(\alpha+1)/2}} + \frac{4\cos^2\phi\cos(2\phi)\Gamma(\alpha+1)}{C_1^2 b^{\alpha+1}}\right\} \quad (31)$$

$$\kappa^*(m,\lambda) = \frac{a}{N\bar{r}^2}\left\{\frac{\Gamma(\alpha+3)}{b^{\alpha+3}} + \frac{C_3\Gamma(\alpha+2)}{C_4^{\alpha+2}} + \frac{C_3^2}{2}\left[\frac{\Gamma(\alpha+1)}{C_4^{\alpha+1}} - \frac{\Gamma(\alpha+1)}{b^{\alpha+1}}\right]\right\} \quad (32)$$

where

$$C_1 = \frac{4\pi}{\lambda}(n-1), \quad C_2 = \frac{b}{C_1} + \tan\phi, \quad C_3 = \frac{\lambda}{4\pi k}, \quad C_4 = b + \frac{2}{C_3}, \quad \psi = \tan^{-1}\frac{1}{C_2} \quad (33)$$

If the imaginary part of the refractive index is very small (of order 0.01), the following equation, obtained from Equation (16), can be used instead of Equation (25):

$$\beta^*(m,\lambda) = \frac{a}{N\bar{r}^2} \times \left\{\frac{2\Gamma(\alpha+3)}{b^{\alpha+3}} - \frac{4\sin[(\alpha+2)\chi]\Gamma(\alpha+2)}{C_1(b^2+C_1^2)^{(\alpha+2)/2}} + \frac{4\Gamma(\alpha+1)}{C_1^2 b^{\alpha+1}} - \frac{4\cos[(\alpha+1)\chi]\Gamma(\alpha+1)}{C_1^2(b^2+C_1^2)^{(\alpha+1)/2}}\right\} \quad (34)$$

where

$$\chi = \tan^{-1}\frac{C_1}{b} \quad (35)$$

(3) *For soot particles.* The Penndorf approximation, Equations (17)–(25), is used to obtain the dimensionless

coefficients for small particles:

$$\beta^*(m,\lambda) = \frac{a}{N\bar{r}^2}\left\{c_1\left(\frac{2\pi}{\lambda}\right)\frac{\Gamma(\alpha+4)}{b^{\alpha+4}} + c_2\left(\frac{2\pi}{\lambda}\right)^3\frac{\Gamma(\alpha+6)}{b^{\alpha+6}} + c_3\left(\frac{2\pi}{\lambda}\right)^4\frac{\Gamma(\alpha+7)}{b^{\alpha+7}}\right\} \tag{36}$$

$$\kappa^*(m,\lambda) = \frac{a}{N\bar{r}^2}\left\{c_1\left(\frac{2\pi}{\lambda}\right)\frac{\Gamma(\alpha+4)}{b^{\alpha+4}} + c_2\left(\frac{2\pi}{\lambda}\right)^3\frac{\Gamma(\alpha+6)}{b^{\alpha+6}} + c_4\left(\frac{2\pi}{\lambda}\right)^4\frac{\Gamma(\alpha+7)}{b^{\alpha+7}} + c_5\left(\frac{2\pi}{\lambda}\right)^5\frac{\Gamma(\alpha+9)}{b^{\alpha+9}} + c_6\left(\frac{2\pi}{\lambda}\right)^7\frac{\Gamma(\alpha+10)}{b^{\alpha+10}}\right\} \tag{37}$$

It is noteworthy that the Penndorf approximation is an extension of the Rayleigh limit approximation

$$\kappa^* = \frac{\kappa}{N\pi\bar{r}^2} = \frac{2\pi a}{N\bar{r}^2}\frac{24nk}{[(n^2-k^2+2)^2+4n^2k^2]}\frac{\Gamma(\alpha+4)}{\lambda b^{\alpha+4}} \tag{38}$$

$$\sigma^* = \frac{\sigma}{N\pi\bar{r}^2} = \frac{2\pi a}{N\bar{r}^2}\frac{8}{3}x^4\left|\frac{m^2-1}{m^2+2}\right|^2\frac{\Gamma(\alpha+4)}{\lambda b^{\alpha+4}} \tag{39}$$

obtained by including higher-order terms in the series expansion of the Mie coefficients. Also,

$$\beta^* = \kappa^* + \sigma^* \tag{40}$$

In addition to the above proposed approximations, there are, as mentioned in the introduction, two other approximations of radiative properties, which have been considered in this study:

(a) *Tien* et al.[4]:

$$Q_\beta = 2[1 - e^{-G\rho}] \tag{41}$$

which gives after integration

$$\beta^* = \frac{2a}{N\bar{r}^r}\left\{\frac{\Gamma(\alpha+3)}{b^{\alpha+3}} - \frac{\Gamma(\alpha+3)}{[4\pi(n-1)G/\lambda+b]^{\alpha+3}}\right\} \tag{42}$$

where

$$G = \frac{6n}{4n^4-8n^3+8n^2+4n+1} \tag{43}$$

and

$$\rho = \frac{4\pi(n-1)r}{\lambda} \tag{44}$$

(b) *Buckius and Hwang*[5]:

$$\left[\frac{\bar{\beta}}{x_{32}F}\right]^{-1} = \frac{1}{24}\left[1+\left(\frac{x_{32}F}{0.016}\right)^2\right]^{-1} + \left[\frac{2.25}{(x_{32}F)^{1.1}}\right]^{-1} \tag{45}$$

$$\left[\frac{\bar{\kappa}}{x_{32}F}\right]^{-1} = \frac{1}{24}\left[1+\left(\frac{x_{32}F}{0.0275}\right)^2\right]^{-1} + \left[\frac{1}{(x_{32}F)^{1.16}}\right]^{-1} \tag{46}$$

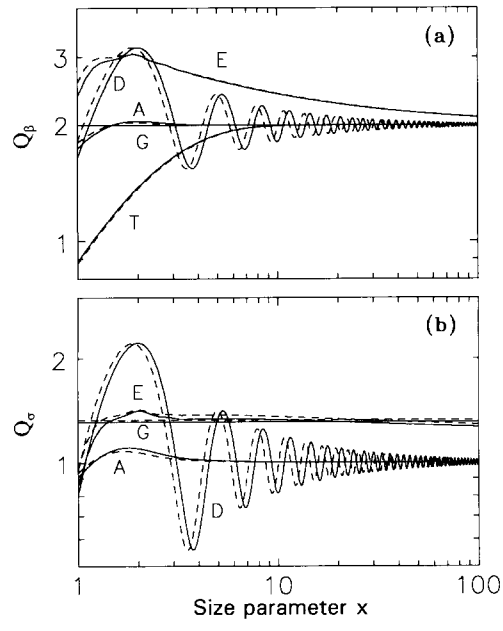

Figure 1 Efficiency factors of coal ($m = 2.02 - 0.8i$, solid line) and char ($m = 2.09 - 0.92i$, dashed line) particles as a function of size parameter (x), as computed by the Mie theory (E) and the geometrical-limit (G), anomalous-limit (A), dielectric limit (D) and Tien *et al.* (T) approximations: a, extinction efficiency factor (Q_β); b, scattering efficiency factor (Q_σ)

where

$$x_{32}F = \frac{\pi}{12\lambda}\frac{\int_0^\infty r^3 n(r)\mathrm{d}r}{\int_0^\infty r^2 n(r)\mathrm{d}r}\mathrm{Im}\left(-4\frac{m^2-1}{m^2+2}\right) \tag{47}$$

and the dimensionless coefficients are defined as

$$\bar{\beta},\bar{\kappa} = \frac{\beta,\kappa}{\int_0^\infty \pi r^2 n(r)\mathrm{d}r} \tag{48}$$

The same particle size distribution, Equations (25)–(27), was used to obtain the radiative coefficients.

Once the radiative properties of each component are found by the approximations, the combined effect of the particle–gas mixture can be obtained by adding their contributions:

$$\bar{\kappa} = \sum_{i=1}^{m}(\bar{\kappa}_\mathrm{p})_i + \sum_{j=1}^{n}(\bar{\kappa}_\mathrm{g})_j \tag{49}$$

where m and n are the numbers of particle types and gas components respectively, and

$$\bar{\beta} = \bar{\kappa} + \sum_{i=1}^{m}(\bar{\sigma}_\mathrm{p})_i \tag{50}$$

RESULTS AND DISCUSSION

Evaluation of the approximations

The approximations proposed above were used to compute the spectral properties of the particle types under consideration, and the results were compared with those obtained from the rigorous Mie theory. The

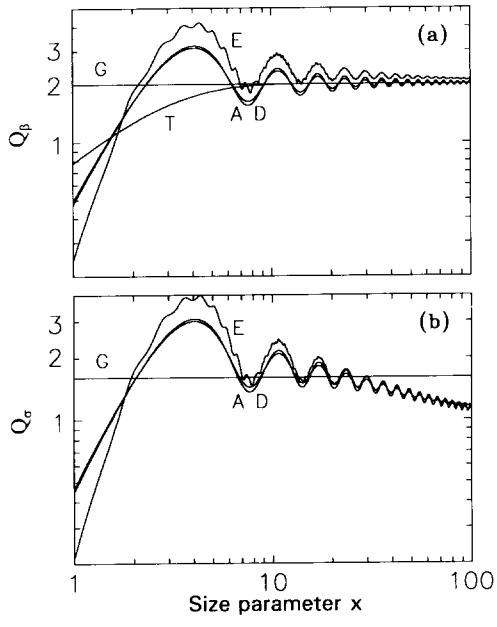

Figure 2 Efficiency factors of fly ash ($m = 1.5 - 0.01i$) as a function of size parameter (x); as computed by the Mie theory (E) and the geometrical limit (G), anomalous-limit (A), dielectric-limit (D) and Tien *et al.* (T) approximations: a, b as in *Figure 1*

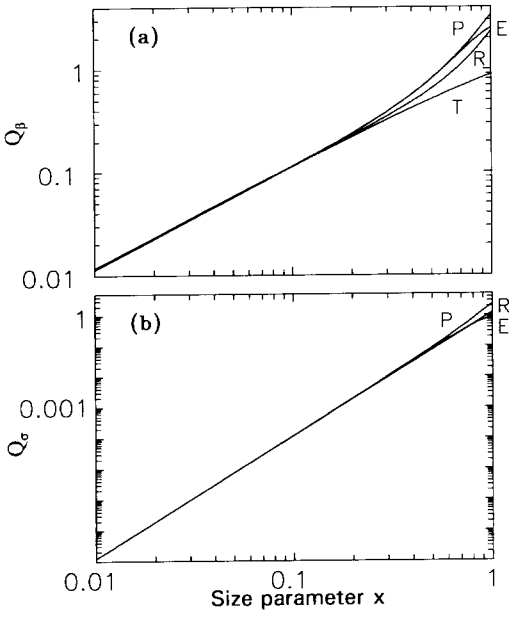

Figure 3 Efficiency factors of soot particles ($m = 1.98 - 0.93i$) as a function of size parameter (x), as computed by the Mie theory (E) and the Penndorf (P), Rayleigh (R), and Tien *et al.* (T) approximations: a, b as in *Figure 1*

tedious and repetitive calculation procedure required for obtaining the Mie coefficients was simplified by using the symbolic language Mathematica (Wolfram Research, Inc.). The calculation of the infinite series of Riccati–Bessel functions was continued until the order of a new term was $<10^{-6}$. The symbolic computation procedure is very simple, and the computing time increases exponentially with the size parameter.

To obtain the best compatibility with the chemical reaction kinetics in the authors' combustor model (below), anthracite was chosen as the coal because it

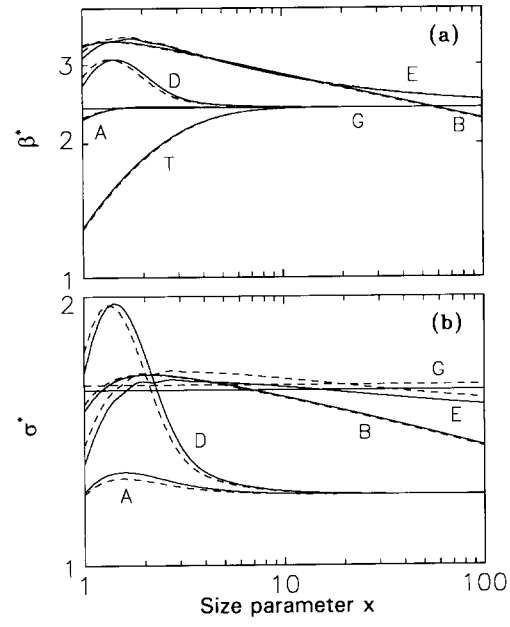

Figure 4 Dimensionless extinction and scattering coefficients of coal ($m = 2.02 - 0.8i$, solid line) and char ($m = 2.09 - 0.92i$, dashed line) particles ($\bar{d} = 100\,\mu$m, $\alpha = 4$) as a function of size parameter (x), as computed by the Mie theory (E) and the geometrical-limit (G), anomalous-limit (A), dielectric-limit (D), Tien *et al.* (T) and Buckius and Hwang (B) approximations: a, dimensionless extinction coefficient (β^*); b, dimensionless scattering coefficient (σ^*)

has the highest C:O and C:H ratios and the least amounts of other elements. *Figure 1a* shows that all approximations of the extinction efficiency factor of coal and char particles (for anthracite, $m = 2.02 - 0.8i$, from ref. 34; for char, $m = 2.09 - 0.92i$, from ref. 32), as well as the exact solution, converge to the 'geometrical limit', where $Q_\beta = 2.0$, as the size parameter x increases. The approximations produce relatively large errors at $x = 1$, of ~15.9%, ~26.5% and ~30.7% for the geometrical, anomalous, and dielectric limits respectively; the error increases and then decreases as x increases. At $x = 100$, for example, the error is 4.6% for the geometrical and anomalous limits, and 4.8% for the dielectric limit. The anomalous limit suggested by Mengüç and Viskanta[10] for coal produces errors of up to 26.5% because of the high refractive index. For particles of moderate size parameter ($1 < x < 27$), none of the approximations gives a good result (the error is >10%), and the general Mie scattering equations must be used.

For the scattering efficiency factor, on the other hand, *Figure 1b* shows that the geometrical limit is a good approximation for $x > 2$, with errors of 7.1% and 3.5% at $x = 2$ and $x = 100$ respectively, and is clearly superior to the other approximations.

For particles with a large size parameter and a low refractive index ($x \gg 1$ and $|m - 1| \ll 1$), such as fly ash ($m = 1.5 - 0.01i$, ref. 35), both the anomalous limit and the dielectric limit exhibit an oscillating pattern similar to the exact Mie solution (*Figure 2*). The errors in the extinction efficiency factor for size parameter $x = 30$ ($d = 20\,\mu$m and $\lambda = 2\,\mu$m) are 7.9% for the anomalous-limit approximation, and 5.3% for the dielectric-limit one. The errors in the scattering efficiency factor are much smaller: 1.0% and 4.8% for the anomalous-limit and dielectric-limit approximations respectively.

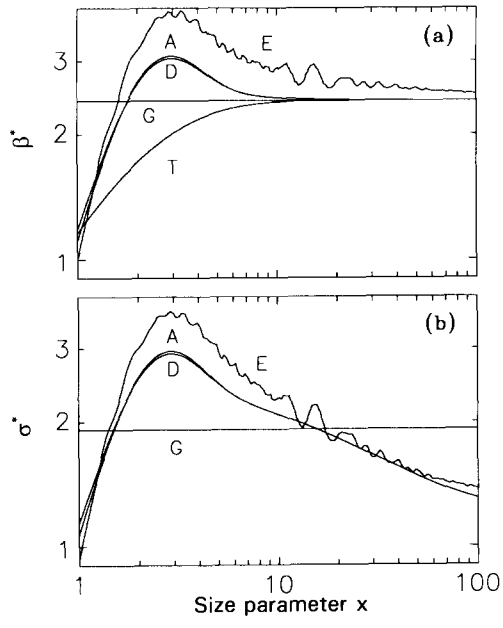

Figure 5 Dimensionless extinction and scattering coefficients of fly ash ($\bar{d} = 20\,\mu$m, $\alpha = 4$, $m = 1.5 - 0.01$i) as a function of size parameter (x), as computed by the Mie theory (E) and the geometrical-limit (G), anomalous-limit (A), dielectric-limit (D) and Tien *et al.* (T) approximations: a, b as in *Figure 4*

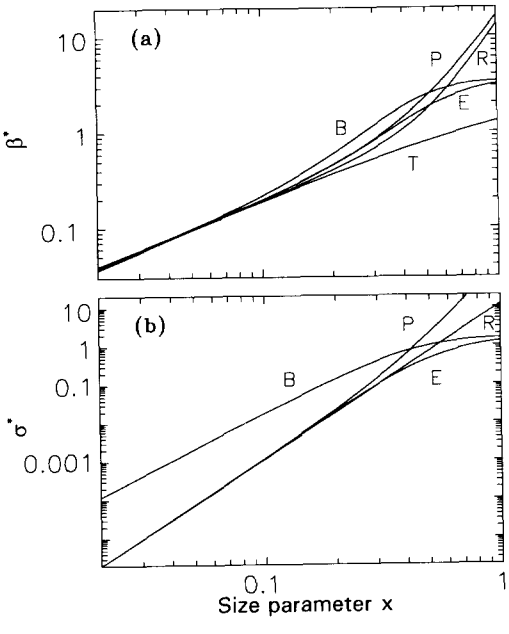

Figure 6 Dimensionless extinction and scattering coefficients of soot particles ($\bar{d} = 0.06\,\mu$m, $\alpha = 3$, $m = 1.98 - 0.93$i) as a function of size parameter (x), as computed by the Mie theory (E) and the geometrical-limit (G), anomalous-limit (A), dielectric-limit (D), Tien *et al.* (T) and Buckius and Hwang (B) approximations: a, b as in *Figure 4*

For soot particles ($m = 1.98 - 0.93$i, ref. 36) of $d = 0.02 - 0.06\,\mu$m, the Penndorf approximation is a good choice: as seen in *Figure 3*, the errors in Q_β and Q_σ for $x = 0.1$ (typical for soot in coal combustors) are 0.003% and 0.08% respectively. At the same x, the Rayleigh approximation and the correlation by Tien *et al.*[4] produce errors of 1.2% and 0.4% respectively in the extinction efficiency factor. The correlation deviates strongly from the exact solution in the medium size-parameter range, because the expression was derived from the Rayleigh limit and interpolated to meet the geometrical limit as $x \to \infty$. The expression is indeed very simple, but its use is thus limited to either very small or large particles. Originally this correlation was developed on the assumption of $n - 1 = k$, which is a reasonable condition for soot particles.

Figures 4–6 show calculations of the dimensionless extinction and scattering coefficients for coal/char, fly ash and soot particles. The approximate solutions were compared with the exact Mie solutions, which were obtained by numerical integration of Equation (2). As seen in *Figure 4a*, the only empirical correlation by Buckius and Hwang[5] predicts values of the extinction coefficient of coal/char particles of moderate size parameter ($1 \leqslant x \leqslant 60$) that compare reasonably with the values obtained from the exact Mie solution, giving an error $\leqslant 5.9\%$. Since the deviation of this approximation from the exact solution increases rapidly beyond $x = 17$, the most simple geometrical-limit approximation is better for particles of larger size parameter ($x > 60$), although the other approximations examined here also give the same results in that range. The geometrical limit produces errors of 5.5% and 4.0% at $x = 60$ and $x = 100$ respectively, and the error decreases as the size parameter increases. Since the size parameter of coal/char particles reaches high values (up to 100π when $d = 100\,\mu$m) in coal combustors, the geometrical limit is suitable for evaluation of their extinction coefficients.

Unlike the situation for the extinction coefficient, *Figure 4b* shows that the correlation of Buckius and Hwang[5] is suitable for calculating the scattering coefficient only in a relatively narrow range of size parameter: the error is limited to 10% only at $42 \leqslant x \leqslant 63$ and the approximation is the best of all in the range of $1 \leqslant x \leqslant 7$, matching the exact solution there within an error of 1.5%. For size parameter $x \geqslant 7$, the geometrical limit should be chosen, with the error increasing to 3.9% at $x = 100$. Owing to the high refractive indices of coal and char, i.e. $|m - 1| \approx 1$, neither the anomalous nor the dielectric limit gives good agreement with the exact solutions for these particles.

For fly ash, the oscillating pattern resulting from solutions using the anomalous- and dielectric-limit approximations (*Figure 2*) matches the exact solution better than do the other approximations, but, as seen in *Figure 5a*, the errors in the extinction coefficient for small size parameter are as large as −20.9% (for the anomalous limit) and −19.9% (dielectric limit). It is noted that, fortuitously, the approximations underestimate the extinction coefficient for clean fly ash, whereas in real combustors the fly ash is usually attached to some unburnt carbon which tends to increase its absorption coefficient. Nevertheless, owing to the relative large error and since only clean fly ash is considered here, and since it is very difficult to predict the amount of attached carbon, the exact solution is recommended at moderate size parameters ($2 \leqslant x \leqslant 30$). For $x > 40$, all the approximations converge to the geometrical limit, with $\leqslant 7\%$ error thereafter until $x = 100$. The trend is similar for the scattering coefficient (*Figure 5b*), but both the anomalous- and dielectric-limit approximations are clearly superior to the geometrical-limit one, producing an error $\leqslant 10\%$ in the discrete ranges $8.6 \leqslant x \leqslant 10.5$, $11.6 \leqslant x \leqslant 14.5$ and $16.2 \leqslant x \leqslant 100$.

As seen in *Figure 6b*, all the approximations for the

Table 1 Range of size parameter x in which each approximation produces an error of $\leqslant 10\%$ in the extinction coefficient β and the scattering coefficient σ

		Coal/char		Ash		Soot	
Approximation	Equation	β	σ	β	σ	β	σ
Geometrical limit	29, 30	23–100[a]	1–100	25–100[a]	12–28	NA[b]	NA
Anomalous limit	31, 32	23–100[a]	NA	25–100[a]	16–100	NA	NA
Dielectric limit	34, 32	23–100[a]	NA	25–100[a]	16–100	NA	NA
Tien *et al.*[4]	42	23–100[a]	ND[c]	25–100[a]	ND	0–0.14	ND
Buckius and Hwang[5]	45, 46	1–100	1–60	28–34	42–63	0–0.08	NA
Rayleigh limit	38, 39	NA	NA	NA	NA	0–0.18	0–0.34
Penndorf[31]	36, 37	NA	NA	NA	NA	0–0.38	0–0.16
Recommended equation(s)		29, 45	30	31, 34	32	36	37, 39

[a] May be used for $x \to \infty$
[b] Not applicable
[c] Not defined for scattering coefficient

extinction coefficient of soot particles are quite accurate at x up to ~0.1, and the Penndorf approximation is the most accurate at x up to ~0.4, where the error is ~ 10%. Its superiority over the Rayleigh approximation, which uses only the first leading term of the series expansion, is simply due to the use of higher-order terms. The other approximations produce much larger errors, of 17.9% (Rayleigh), 36.0% (Tien *et al.*[4]) and 43.2% (Buckius and Hwang[5]). Although x for soot particles in coal combustors is $\not> 0.2$, at which level the errors produced by the other approximations become smaller, it is clear from *Figure 6a* that the Penndorf approximation is still the best, producing a maximum error of 0.3% at $x = 0.2$. For the scattering coefficient (*Figure 6b*), on the other hand, the Rayleigh approximation is better than the Penndorf approximation, with errors of 4.7% and 13.0% respectively at $x = 0.2$. It is in any case noteworthy that the single-scattering albedo $\omega \leqslant 0.044$ at $x \leqslant 0.2$, and that scattering by soot particles is therefore practically negligible.

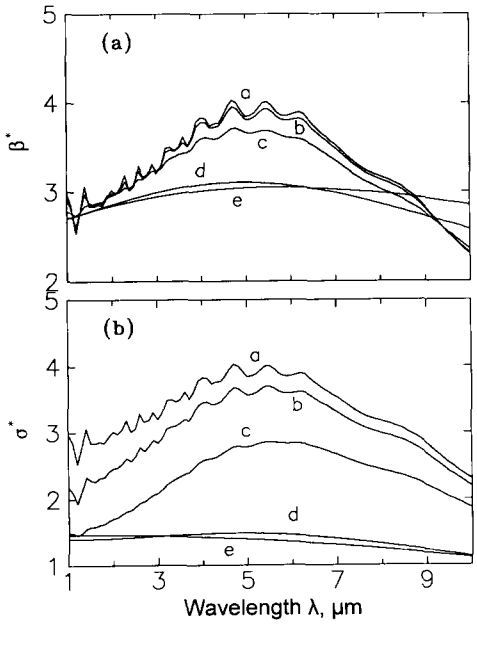

Figure 7 Spectral effect of refractive index on the dimensionless extinction and scattering coefficients of fly ash for $n = 1.5$ and $k =$ (a) 0, (b) 0.01, (c) 0.05, (d) 0.307, (e) 0.6

To facilitate the choice of approximations for computing the radiative coefficients of the particles in coal combustors, a summary of the size-parameter ranges in which the approximations produce an error <10% is given in *Table 1*.

Uncertainty in the complex refractive index and its effect on the properties

For both fundamental and practical reasons it is of interest to examine the effect of the magnitude of the complex refractive index of the particles on the values of the extinction and scattering coefficients. A case in point, examined below, is that many different values of the complex refractive index of ash are to be found in the literature[37], with the absorptive index k varying from 0.005 to 0.6 and the refractive index n from 1.4 to 1.7. Fly ash was chosen for examination because it can significantly affect radiative heat transfer in coal combustors, and the uncertainty in its complex index could create unacceptable errors in predicting heat transfer and consequently combustor performance and emissions.

Using the exact Mie equations, a comparison of the extinction and scattering coefficients was made for several different values of k, including the dielectric case ($k = 0$), with $n = 1.5$. The results are shown in *Figure 7*. For low absorptive indices, $k \leqslant 0.01$ (cases a and b), sharp oscillations are observed in the short-wavelength region ($\lambda < 6\,\mu$m), requiring high computational resolution. The oscillations disappear at longer wavelength or for higher absorptive indices. In general, the effect of k on the extinction coefficient peaks at $\lambda = 4.7\,\mu$m, reducing the extinction coefficient by 2% for a fivefold increase in k (from 0.01 to 0.05) at that wavelength. At the wavelength typical of radiation in pulverized coal combustors, $\lambda = 2\,\mu$m, the effect of k, throughout the range investigated, on the extinction coefficient is only 5.7%. However, its influence on the scattering coefficient is 40.5%, owing to the consequent increase of two orders of magnitude in the absorption coefficient as k increases. Further analysis of the sensitivity of the radiative properties to the refractive index for particles of small size parameter can be found in the paper by Kim *et al.*[38].

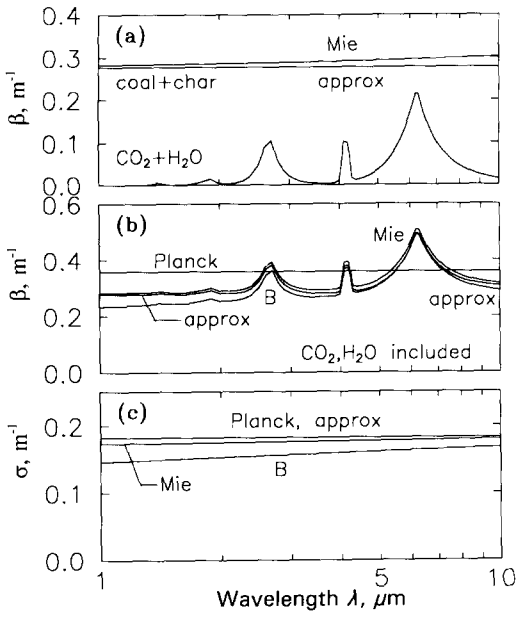

Figure 8 Spectral extinction and scattering coefficients of the particle–gas mixture (coal + char + CO_2 + H_2O, 50% of coal mass devolatilized) in the combustor pre-ignition zone. For the particulate components, comparative computations were made by the Mie theory (Mie), the combination of the proposed approximations (approx) and the Buckius and Hwang correlation (B). The radiative coefficients of the gas components were always computed by the exponential wide-band model. a, Contributions of the individual mixture components to the spectral extinction coefficient; b, spectral extinction coefficient of the mixture; c, spectral scattering coefficient of the mixture

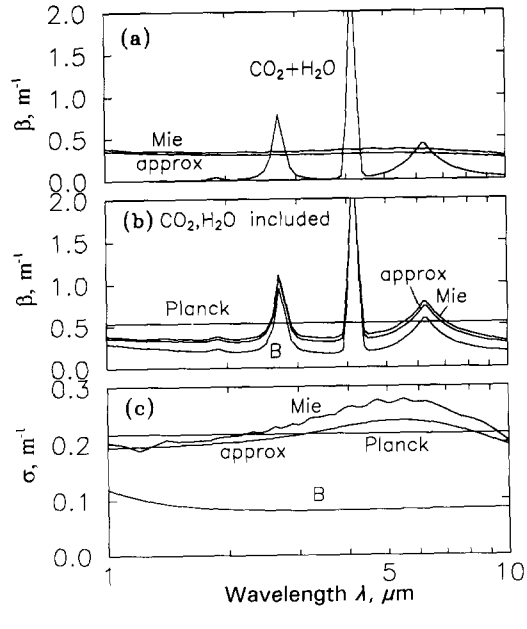

Figure 9 Spectral extinction and scattering coefficients of the particle–gas mixture (char + ash + CO_2 + H_2O, 50% of char burnt) in the combustor flame zone. Computations and a, b, c as in *Figure 8*

Radiative properties of the particle–gas mixture

The spectral extinction and scattering coefficients of the entire particle–gas mixture in a coal combustor, in the wavelength range 1–10 μm typical of the interior of such a combustor, were compared by computing the particulate-component coefficients by a combination of the above approximations, summarized in *Table 1* and Equations (29)–(32), (36) and (37), by the Mie theory and by the correlation suggested by Buckius and Hwang[5]. The results for the pre-ignition zone are shown in *Figure 8* and for the flame zone in *Figure 9*. The radiative coefficients of the gaseous components were computed by the exponential wide-band model, Equation (1). *Figures 8* and *9* also show a comparison with the Planck mean absorption coefficient computed from

$$\bar{\beta} = \frac{\int_0^\infty \beta I_b d\lambda}{\int_0^\infty I_b d\lambda} = \frac{15}{\pi^4}\int_0^\infty \frac{\beta \xi^3}{e^\xi - 1} d\xi \qquad (51)$$

where $\xi = 14388/\lambda T$ and I_b is Planck's black-body function. β is computed by the approximations. The coal was taken to be dry, ash-free anthracite (initial mass concentration 0.01 kg m^{-3}) with particle size characterized by $\bar{d} = 100\,\mu$m and $d_m = 80\,\mu$m. In practice, typically 70–80% of the coal particles pass through a 74 μm screen[39], but larger particles were used both in the present work (100 μm) and by others[28] (90–106 μm). This anthracite was assumed to have a volatile matter of 7.3 wt%, an elemental composition (wt%) of 93.5 C, 2.6 H, 2.3 O and 0.9 N, and a refractive index $m = 2.02 - 0.80i$. The refractive index of char was taken as $m = 2.09 - 0.92i$. It was assumed that four ash particles of $\bar{d} = 20\,\mu$m and 350 smaller particles of $\bar{d} = 5\,\mu$m, all having a refractive index $m = 1.5 - 0.01i$, were produced from each coal particle. Since no size distribution data for the ash particles were available, the same distribution as that of the coal was assumed. The soot particles were characterized by $\bar{d} = 0.06\,\mu$m, $d_m = 0.045\,\mu$m and $m = 1.98 - 0.93i$.

The explanation of *Figures 8* and *9* is as follows. As coal particles approach the flame zone, char particles are produced by devolatilization. The volatile matter burns immediately in the gas phase, and accordingly the concentrations of CO_2 and H_2O increase. The contribution of the gas components, especially water vapour, to the radiative properties of the mixture is prominent, as clearly seen in *Figures 8* and *9*. To calculate the radiative properties in the pre-ignition zone, it was assumed that 50% of the coal consists of volatile combustible matter which is released and burnt to CO_2 and H_2O. Given the initial mass concentration of the coal, the concentration of each component in the pre-ignition zone is thus determined to be: CO_2 0.01467 kg m^{-3}; H_2O 0.00117 kg m^{-3}; coal 0.005 kg m^{-3}; and char 0.00483 kg m^{-3}. Since the geometrical limit is used for coal and char particles, their contribution to the radiative coefficients is constant throughout the wavelength range considered here, as seen in *Figure 8a*. The geometrical limit yields a lower value for the extinction efficiency factor than the Mie result, especially at longer wavelengths, and thus the extinction coefficient is underestimated through the combined approximation by 3.0%, 4.9% and 6.3% at $\lambda = 2$, 5 and 8 μm respectively (*Figure 8b*). The empirical correlation of Buckius and Hwang[5] generally yields lower values (12.4%, 5.8% and 3.4% errors at the same wavelengths). Similar results were obtained for the scattering coefficient (*Figure 8c*), with the approximations producing errors of 4.3%, 2.8% and 1.8% and the Buckius

and Hwang[5] correlation producing errors of 12.8%, 9.2% and 7.6% for the respective wavelengths. Since scattering by gas components is usually neglected, there is no effect of CO_2 and H_2O on the scattering coefficient.

It is to be noted that Planck's mean absorption coefficient may differ from the average of the spectral properties computed by the approximations and the Mie equations and shown in *Figures 8* and *9*, because the spectral properties here are computed only in the $1-10\,\mu m$ wavelength region, so the contributions from the absorption bands of the gases and the variation of the properties of the particles outside this wavelength region (especially the $15\,\mu m$ band of CO_2 and the increase in the extinction coefficient of soot $<1\,\mu m$) do not appear in the figures. Since the radiation in coal combustors is most intense at $\lambda \approx 2\,\mu m$, the effects of such bands are not significant in overall radiative transfer. Planck mean coefficients, on the other hand, are obtained by integration over the entire spectrum (Equation 51) and thus include the contributions of wavelength bands outside the $1-10\,\mu m$ range shown in *Figures 8* and *9*.

As combustion continues, the effect of large particles decreases. While the number of coal and char particles decreases in the flame region, that of ash and soot particles increases. On the assumption that 50% of the char is completely burnt, the concentration of both char and ash particles in the flame zone is taken to be $0.00483\,kg\,m^{-3}$, and the volume fraction of the soot particles, in the absence of specific information for anthracite, was chosen to be 7.0×10^{-8}, at the lower end of soot concentrations reported[40] for fires of various combustibles. The concentrations of CO_2 and H_2O also increase further to 0.01729 and $0.00234\,kg\,m^{-3}$ respectively in the flame zone, as a result of the oxidation of carbon and hydrogen.

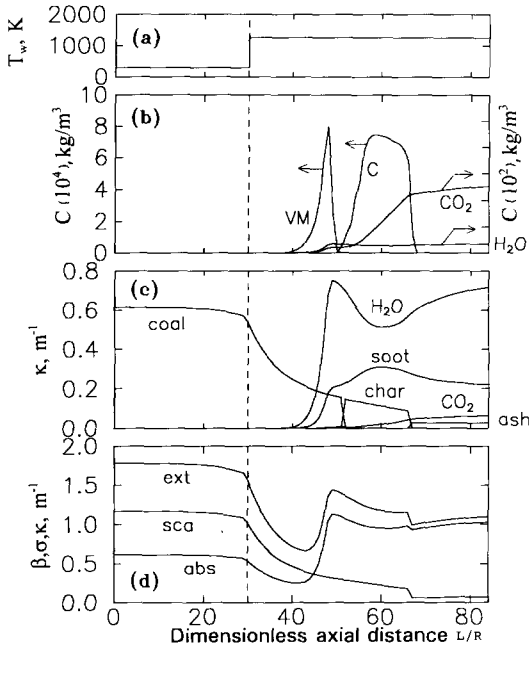

Figure 10 Axial distributions of component concentrations, component contributions to the Planck mean absorption coefficient, and Planck mean absorption, scattering and extinction coefficients of the entire mixture. a, Temperature profile along the combustor wall; b, concentrations of the mixture components; c, contributions of each mixture component to the Planck mean absorption coefficient; d, Planck mean absorption (abs), scattering (sca), and extinction (ext = abs + sca) coefficients

The contributions from each component to the scattering coefficient, as well as the extinction and scattering coefficients for the entire mixture, are shown in *Figure 9*. Although the peak is not shown to full extent in *Figure 9a* and *b*, the extinction coefficient in the flame zone reaches almost $12\,m^{-1}$ owing to the $4.3\,\mu m$ absorption band of CO_2. Whereas the approximations produce 8.9%, 11.0% and 9.1% errors at $\lambda = 2$, 5 and $8\,\mu m$ respectively in the extinction coefficient (*Figure 9b*), the Buckius and Hwang[5] correlation gives much higher errors, 43.1%, 46.3% and 39.2% at the same wavelengths. Using the approximations, the errors in the scattering coefficient (*Figure 9c*) at the same wavelengths are 5.1%, 11.5% and 9.3%, whereas the Buckius and Hwang[5] correlation gives errors of 61.2%, 7.0% and 65.7%. Since the major deviation of this empirical correlation from the Mie results occurs in the scattering coefficient, it gives slightly better results for the prediction of the absorption coefficient, with errors of 11.8% in the pre-ignition zone and 13.8% in the flame zone, both at $\lambda = 2\,\mu m$. The approximations produce 14.2% and 15.1% errors in the same regions at the same wavelength.

Effect of the approximation errors on the temperature and radiation fields in a pulverized coal combustor

In addition to the above evaluation of the suitability of simplified expressions for determining radiative properties, it is also of interest to evaluate the effect of errors and uncertainties in these properties on the overall behaviour of pulverized coal combustors. This analysis was performed by computing the temperature and radiation intensity distributions along such a combustor with radiative properties varied by ±5% and ±10% from the values determined by the approximations. The computation was made using a comprehensive numerical model developed by the authors[41], which considers the heat transfer, fluid mechanics and reaction kinetics in such a combustor. The combustor concerned is a vertical, well-insulated refractory drop-tube, 2.13 m long and 5.08 cm i.d. The coal burnt is anthracite (VM 10.8 wt% db, ash 20.6 wt% db, gross CV $27.73\,MJ\,kg^{-1}$), of particle size $\bar{d} = 100\,\mu m$, fed at $90\,mg\,s^{-1}$; 100% excess air is provided. A step temperature distribution along the interior surface, with $T = 294\,K$ over the first 36% of the tube length and $T = 1255\,K$ over the remainder (*Figure 10a*), was assigned as a boundary condition typical of experimental data for this combustor.

Figure 10b shows the axial concentration profiles of the combustion reactants and products, as computed by the model[41]. *Figure 10c* shows the axial distribution of the contributions of the individual components to the absorption coefficient. As combustion commences, water vapour, CO_2, and soot and ash particles are produced. It is noted again that although some other gases, in particular CO, may affect the radiative properties of the mixture, the only gases considered in this radiative transport model, in consonance with most other coal combustion models, were water vapour and CO_2. *Figure 10c* shows that whereas only the coal particles determine the radiative properties of the mixture in the pre-ignition zone, the water vapour and

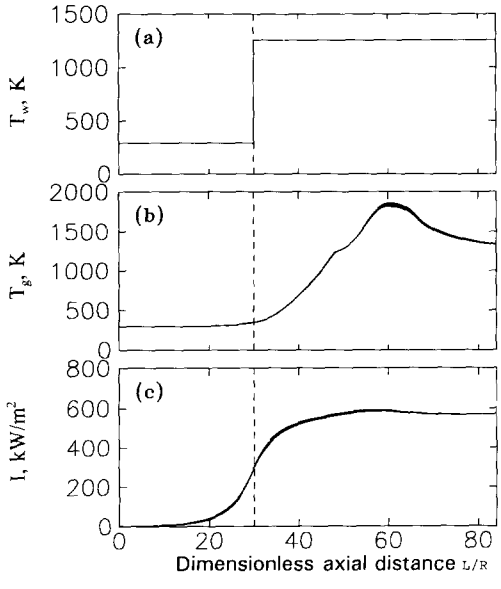

Figure 11 Axial distributions of the wall and gas temperatures and of the radiation intensity in the combustor. a, Wall temperature distribution; b, radially averaged gas temperature distributions for ±5% and ±10% variations in the radiative properties; c, radiation intensity distribution and its variation for ±5% and ±10% variations in the radiative properties

soot have the dominant effect on the radiative properties in the flame zone (contributing 69.7% and 21.4% respectively to the total absorption coefficient at the exit of the combustor). It is hence noteworthy that proper accounting of the concentration distribution and radiative properties of these components is important for characterizing flame and combustor behaviour. The axial distribution of the absorption, scattering and extinction coefficients of the entire mixture is shown in *Figure 10d*. The gradual decrease in these coefficients near the middle section of the combustor is primarily due to the velocity increase as the particles approach the flame front, causing a reduction in their number density.

The gas temperature and radiation intensity distributions are shown in *Figure 11*. It was found that a ±5% variation in the radiative properties resulted in only 0.48–1.05% change in the gas temperature and 0.36–0.54% change in the radiation intensity. A ±10% variation in the radiative properties resulted in a change of 0.91–1.45% in the gas temperature and 0.72–0.9% change in the radiation intensity. When the magnitudes of the properties decrease, i.e. the medium becomes optically thinner, more radiation energy is transferred from the flame zone to the pre-flame zone, increasing the radiation intensity in the pre-flame zone and decreasing that in the flame zone. Since the approximations proposed in this study produce errors of ~2–9% at $\lambda = 2\,\mu$m (*Figures 7* and *8*), the combustor analysis indicates that the use of these approximations produces negligible errors in the modelling presented here, at least when the coal is anthracite. The suitability of these approximations for modelling the combustion of other coals, as well as to coal combustion processes in which radiative-property-altering quantities of CO and hydrocarbon gases are present, remains to be explored but is not expected to change significantly.

CONCLUSIONS AND RECOMMENDATIONS

The high computational effort associated with the solution of the Mie equation has often forced the use of extreme assumptions which simplify the computation of the radiative properties but introduce large (or unknown) errors in the analysis and modelling of heat transfer and combustion in high-temperature particle–gas mixtures.

A number of approximate expressions for calculating these coefficients for each of the particulate types, which require a small fraction of a second on a 66 MHz PC, were examined here in a wide range of size-parameters by comparison to the results of the full Mie equations. A set of these approximations, which typically produce overall errors of less than 8.9% and 5.1% in the spectral extinction and scattering coefficients, respectively, was selected and recommended for use for the combustion reactants and products in pulverized coal combustors, as characterized by composition, particle sizes, and refractive indices. The more specific major conclusions are:

1. For pulverized coal and char particles of moderate size parameter ($1 \leqslant x \leqslant 60$), the empirical correlation of Buckius and Hwang[5], Equation (45), is a good approximation (error $\leqslant 5.9\%$) for the extinction coefficient. For particles of larger size parameter, the geometrical-limit approximation, Equation (29), is recommended (error 5.5% at $x = 60$, 4.0% at $x = 100$). For the scattering coefficient for coal/char particles, the geometrical-limit approximation, Equation (30), is good up to $x = 100$, with error $\leqslant 3.9\%$.
2. For fly ash particles, either the anomalous-limit approximation, Equations (31) and (32), or the dielectric-limit approximation, Equation (34), is recommended (for $x \geqslant 30$, the error in the extinction coefficient is $\leqslant 6.0\%$ and the error in the scattering coefficient is $\leqslant 1.9\%$). For particles of smaller size parameter ($x \leqslant 30$) however, the approximations produce errors which increase to 20% as x decreases to 6. If higher accuracy is needed in this range, the exact Mie solution should be used.
3. For soot particles, the Penndorf approximation[31], Equations (36) and (37), gives accurate results for the extinction coefficient (0.27% error at $x = 0.2$), but the Rayleigh-limit approximation is better for the scattering coefficient (error $\leqslant 4.7\%$ at $x \leqslant 0.2$). It is noted that scattering by soot particles is usually neglected because typically $\omega \leqslant 0.044$.
4. The use of the proposed approximations thus produces an error of $<10\%$ in the radiative properties in both the pre-flame and flame zones in a pulverized anthracite combustor, which generates a negligible error in the gas temperature and radiation intensity predictions.

ACKNOWLEDGEMENT

A supercomputer time grant by the Pittsburgh Supercomputing Center was used for some of the work in this study.

REFERENCES

1 Mie, G. A. *Ann. Phys.* 1908, **25**, 377

2 Dave, J. V. Report 320-3237, IBM Palo Alto Scientific Center, 1968
3 Wiscombe, W. J. NCAR Technical Note NCAR/TN-140+STR, 1979
4 Tien, C. L., Doornink, D. G. and Rafferty, D. A. *Combust. Sci. Technol.* 1972, **6**, 55
5 Buckius, R. O. and Hwang, D. C. *J. Heat Transfer* 1980, **102**, 99
6 Viskanta, R., Ungan, A. and Mengüç, P. M. ASME Paper 81-HT-24, 1981
7 Wall, T. F., Lowe, A., Wibberley, L. J., Mai-Viet, T. and Gupta, R. P. *Combust. Sci. Technol* 1981, **26**, 107
8 Grosshandler, W. L. and Monteiro, S. L. P. *J. Heat Transfer* 1982, **104**, 587
9 Van de Hulst, H. C. 'Light Scattering by Small Particles', Wiley, New York, 1957
10 Mengüç, M. P. and Viskanta, R. *Combust. Sci. Technol.* 1985, **44**, 143
11 Sarofim, A. F. and Hottel, H. C. In 'Sixth International Heat Transfer Conference', Vol. 6, 1978, p. 199
12 Edwards, D. K. 'Advances in Heat Transfer', Academic Press, 1976
13 Modak, A. T. *J. Quant. Spectrosc. Radiat. Transfer* 1979, **21**, 131
14 Mengüç, M. P. PhD Thesis, Purdue University, 1985
15 Tiwari, S. N. *Int. J. Heat Mass Transfer* 1977, **20**, 741
16 Wassel, A. T. and Edwards, D. K. *J. Heat Transfer* 1974, **96**, 21
17 Wassel, A. T. and Edwards, D. K. *J. Heat Transfer* 1976, **98**, 101
18 Tabanfar, S. and Modest, M. F. *J. Heat Transfer* 1987, **109**, 478
19 Edwards, D. K. and Balakrishnan, A. *Int. J. Heat Mass Transfer* 1973, **16**, 25
20 Kerker, M. 'The Scattering of Light', Academic Press, New York, 1969
21 Chylek, P., Grams, G. W. and Pinnick, R. G. *Science* 1976, **193**, 480
22 Flagan, R. C. Paper 77-4, Spring Meeting, Western Section, The Combustion Institute, Seattle, WA, 1977
23 Smoot, L. D. and Pratt, D. T. 'Pulverized-Coal Combustion and Gasification', Plenum Press, New York, 1979
24 Modest, M. F. 'Radiative Heat Transfer', McGraw-Hill, New York, 1993
25 Wiscombe, W. J. *Appl. Optics* 1980, **19**, 1505
26 Sarofim, A. F., Howard, J. B. and Padia, A. S. *Combust. Sci. Technol.* 1977, **16**, 187
27 Helble, J. J., Neville, M. and Sarofim, A. F. In 'Twenty-first Symposium (International) on Combustion', The Combustion Institute, Pittsburgh, PA, 1986, p. 411
28 Helble, J. J. and Sarofim, A. F. *Combust. Flame* 1989, **76**, 183
29 Brewster, M. Q. and Kunitomo, T. In Proceedings, ASME–JSME Thermal Engineering Joint Conference, Vol. 4, 1983, p. 21
30 Brewster, M. Q. and Kunitomo, J. *J. Heat Transfer* 1984, **106**, 678
31 Penndorf, R. B. *J. Opt. Soc. Am.* 1962, **52**, 896
32 Blokh, A. G. 'Heat Transfer in Steam Boiler Furnaces', Hemisphere Publishing, 1988
33 Dunn-Rankin, D. and Kerstein, A. R. *Combust. Flame* 1987, **69**, 193
34 Blokh, A. G. and Burak, L. D. *Therm. Eng.* 1973, **20**, 65
35 Foster, P. J. and Howarth, C. R. *Carbon* 1968, **6**, 719
36 Mackowski, D. W. *Combust. Sci. Technol.* 1987, **53**, 399
37 Gupta, R. P and Wall, T. F. *Combust Flame* 1985, **61**, 145
38 Kim, C., Lior, N. and Okuyama, K. In 'Radiative Heat Transfer: Current Research' (Eds Y. Bayazitoglu, A. L. Crosbie, P. D. Jones, R. D. Scopycec, T. F. Smith, T. W. Wong and S. T. Thynell), HTD-Vol. 276, ASME, New York, 1994, p. 131
39 Singer, J. G. 'Combustion: Fossil Power Systems', 3rd edn, Combustion Engineering, 1981
40 Bard, S. and Pagni, P. J. *J. Heat Transfer* 1981, **103**, 357
41 Kim, C. and Lior, N. ASME Paper 93-WA/HT-37, 1993

NOMENCLATURE

a coefficient in particle size distribution
a_n Mie coefficient
b exponent in particle size distribution
b_n Mie coefficient
C concentration ($kg\,m^{-3}$)
d diameter of particle (μm)
I radiation intensity ($kW\,m^{-2}\,\mu m^{-1}$)
I_b Planck's black-body function ($kW\,m^{-2}\,\mu m^{-1}\,s^{-1}$)
k absorptive index
L combustor tube length (m)
N total number of particles in unit volume (m^{-3})
m complex refractive index, $= n - ik$
n refractive index
Q radiation efficiency factor
R inside radius of combustor tube (m)
r radius of particle (μm)
T temperature (K)
x size parameter, $\pi d/\lambda$
α integrated band intensity ($m\,kg^{-1}$) or size distribution parameter
β extinction coefficient, $= \kappa + \sigma$ (m^{-1})
Γ gamma function
κ absorption coefficient (m^{-1})
λ wavelength (μm)
ν wavenumber (m^{-1})
ρ mass density ($kg\,m^{-3}$)
σ scattering coefficient (m^{-1})
ω single scattering albedo, $= 1 - \kappa/\beta$, or band wing decay width (m^{-1})

Subscripts
g gas
m modal size
p particle
w wall

Superscript
* dimensionless parameter